Available online at www.sciencedirect.com
ScienceDirect
Nuclear Physics A 856 (2011) 46–54
NUCLEAR PHYSICS A
www.elsevier.com/locate/nuclphysa

Study of ^{9}Be + ^{12}C elastic scattering at energies near the Coulomb barrier

R.A.N. Oliveira [a,*], N. Carlin [a], R. Liguori Neto [a], M.M. de Moura [a], M.G. Munhoz [a], M.G. del Santo [b], F.A. Souza [a], E.M. Szanto [a], A. Szanto de Toledo [a], A.A.P. Suaide [a]

[a] *Instituto de Física, Universidade de São Paulo, CEP 66318, 05315-970, São Paulo, SP, Brazil*
[b] *National Superconducting Cyclotron Laboratory, Michigan State University, East Lansing, MI, United States*

Received 15 September 2010; received in revised form 7 February 2011; accepted 17 February 2011

Available online 23 February 2011

Abstract

In this work, angular distribution measurements for the elastic channel were performed for the ^{9}Be + ^{12}C reaction at the energies $E_{Lab} = 13.0$, 14.5, 17.3, 19.0 and 21.0 MeV, near the Coulomb barrier. The data have been analyzed in the framework of the double folding São Paulo potential. The experimental elastic scattering angular distributions were well described by the optical potential at forward angles for all measured energies. However, for the three highest energies, an enhancement was observed for intermediate and backward angles. This can be explained by the elastic transfer mechanism.

Keywords: NUCLEAR REACTIONS ^{12}C(^{9}Be, ^{9}Be), $E = 13.0$, 14.5, 17.3, 19.0, 21.0 MeV; measured E(particle), I(particle), $\sigma(\theta)$; deduced deformation parameters, reaction mechanism features. Comparison with optical model calculations using the São Paulo potential and other data

1. Introduction

In the last few years, nuclear reactions involving weakly bound nuclei became a subject of interest due to the observation of flux enhancement for processes like nucleon transfer and breakup.

* Corresponding author. Tel.: +55 11 3091 7072; fax: +55 11 3031 2742.
E-mail address: rnegrao@dfn.if.usp.br (R.A.N. Oliveira).

0375-9474/$ – see front matter
doi:10.1016/j.nuclphysa.2011.02.005

Through the study of these processes [1–3], it is possible to obtain information about nuclear structure, such as single-particle states and nuclear cluster structure, as well as information about the influence of continuum states in the nuclear reaction dynamics [4–6]. Additionally, the investigation on how these properties change from the stability line to regions far from the stability valley can also be addressed.

In this context, the elastic scattering measurement and coupled channel analysis [7] are very important tools to investigate nucleon transfer and breakup, as they appear as competing mechanisms in the reproduction of the measured angular distributions.

In this work, elastic scattering cross section measurements were performed for the $^{9}\mathrm{Be} + {}^{12}\mathrm{C}$ reaction to study anomalies [7–9] in the extracted optical parameters values and the contribution of inelastic channels, transfer and compound nucleus formation in the elastic scattering process. The experimental data show an enhancement in the elastic cross sections at intermediate and backward angles. This behavior is typically observed in systems where projectile and target present the same core structure [8–10]. This effect can be understood in terms of a $^{3}\mathrm{He}$ transfer process, assuming that $^{12}\mathrm{C}$ has a $^{3}\mathrm{He} + {}^{9}\mathrm{Be}$ cluster structure.

The elastic scattering angular distributions were analyzed in a four steps procedure. Distinctively of previous works, our experimental elastic scattering data have been compared to optical model predictions using a empirical double folding potential [11]. In this process, the normalization parameters for the real and imaginary potentials were adjusted to describe the data at forward angles ($\theta_{CM} \leqslant 80^{\circ}$). The normalization of the real part of the potential shows a decrease as a function of the bombarding energy, and the normalization of the imaginary part of the potential is approximately constant. During the following two steps, we investigate the importance of the coupling to inelastic and transfer channels respectively, and finally in the fourth step we analyse the compound elastic contribution.

2. Experimental setup

The experiment was performed at the University of São Paulo Physics Institute. The $^{9}\mathrm{Be}$ beam was delivered by the 8UD Pelletron accelerator with energies $E_{Lab} = 13.0$, 14.5, 17.3, 19.0 and 21.0 MeV ($E_{CM} = 7.4$, 8.3, 9.9, 10.8 and 12.0 MeV respectively) and hit a 40 $\mu g/cm^2$ thick $^{12}\mathrm{C}$ target. The charged particles produced in the $^{9}\mathrm{Be} + {}^{12}\mathrm{C}$ reaction were detected by means of 13 triple telescopes [12] separated by $\Delta\theta = 10^{\circ}$ in the reaction plane, which covered the angular range from $\theta = 10^{\circ}$ to $\theta = 140^{\circ}$.

The triple telescopes were composed of an ionization chamber, filled with 20 torr of isobutane gas, followed by a 150 μm silicon detector and a 40 mm CsI scintillator crystal. The identification of the elastic events was done by means of two-dimensional spectra like the one shown in Fig. 1(a). The elastic yields were obtained by projecting the $Z = 4$ region on the E_{Si} axis (energy measured by the Silicon detector) and identifying the elastic processes as shown in Fig. 1(b).

As illustrated in this figure, we can see a considerable number of events due to target contamination. In order to subtract the contributions in the energy spectra from this target contamination, we have assumed Rutherford scattering for the involved cross sections. This is a good approximation in our experimental conditions.

The uncertainties in the differential cross section were estimated considering the statistical uncertainty in the yield and the systematic uncertainty of 5% in the target thickness.

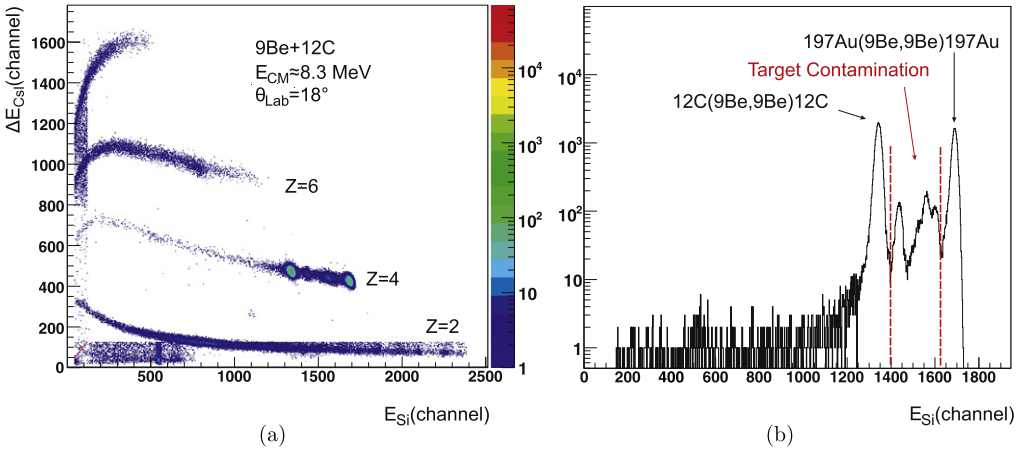

Fig. 1. (Color online.) (a) Two-dimensional spectra of ΔE_{gas} (energy measured by the Gas detector) vs E_{Si} at $E_{CM} = 8.3$ MeV and (b) $Z = 4$ events projection on the energy axis.

3. Data analysis and discussion

3.1. Optical model calculations

In the present work, the experimental data were analyzed using the FRESCO code [13] in the framework of the São Paulo potential (SPP) [11] due to the recent success of this approach in describing nuclear reactions involving weakly bound nuclei [14,15]. Clearly, there are other options for the scattering potential, as shown in recent works by A.T. Rudchick et al. [9] and J. Carter et al. [8] who have used a Woods–Saxon shape and a double folding potential, respectively, and the effects of coupled channels to describe the $^{9}\mathrm{Be} + {}^{12}\mathrm{C}$ scattering data.

For the São Paulo potential, the radial dependence is a folding potential and the energy dependence takes non-local effects into account, in the form

$$V(R, E) = V_F(R) \exp\left(-4\beta^2\right), \tag{1}$$

where $\beta = v/c$, v is the local relative velocity between the two nuclei and $V_F(R)$ is a folding potential obtained by using the matter distributions of the nuclei involved.

In detail, the folding potential depends on the matter densities in the form

$$V_F(R) = \int \rho(\vec{r}_1)\rho(\vec{r}_2) v_{nn}(\vec{R} - \vec{r}_1 - \vec{r}_2)\, d^3r_1\, d^3r_2 \tag{2}$$

where $v_{nn}(\vec{R} - \vec{r}_1 - \vec{r}_2)$ is a physical nucleon–nucleon interaction given by

$$v_{nn}(\vec{R} - \vec{r}_1 - \vec{r}_2) = V_0 \delta(\vec{R} - \vec{r}_1 - \vec{r}_2) \tag{3}$$

with $V_0 = -456$ MeV fm^3 and the usage of a delta function corresponds to the zero range approach. Extensive systematics were performed in Ref. [11], to provide a good description of matter and charge distribution.

In the present work, we adopt the matter and charge diffuseness $a_m = 0.53$ fm and $a_c = 0.56$ fm respectively, and the matter and charge distribution radius given by $R_M = 1.31A^{1/3} - 0.84$ and $R_C = 1.76Z^{1/3} - 0.96$ respectively. In this first step of the analysis, we considered

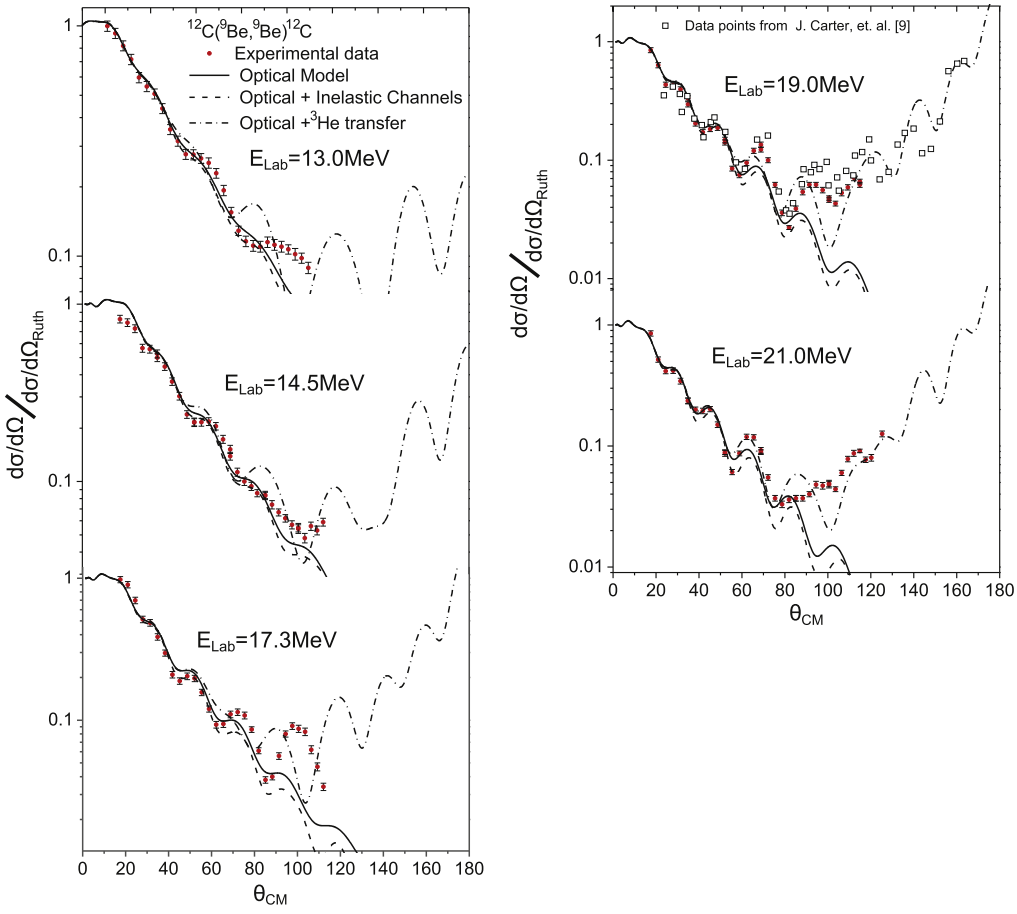

Fig. 2. (Color online.) Angular distributions for the ^{9}Be + ^{12}C system at $E_{Lab} = 13.0$, 14.5, 17.3, 19.0 and 21.0 MeV. The solid lines correspond to optical model fits, the dashed and dash dotted lines represent the same optical potential including the inelastic and elastic transfer mechanisms respectively.

the real and imaginary potential normalizations as free parameters that are adjusted in order to describe the forward angles of the angular distribution ($\theta_{CM} \leqslant 80°$). In this case the nuclear potential is given by the equation

$$V_{SPP} = (N_r + i N_i) V_F(R) \exp\left(-4\beta^2\right), \tag{4}$$

where the normalization coefficients N_r and N_i are reaction energy dependent. The results for the first step are shown as solid lines in Fig. 2. We observe a good agreement for the forward angular region. However, a pronounced disagreement at backward angles for 17.3, 19.0 and 21.0 MeV, is an indication of the importance of other reaction mechanisms, not taken into account in the optical potential. For 13.0 and 14.5 MeV, the optical model description is reasonable. Finally, Fig. 2 also shows an angular distribution for $E_{Lab} = 19.0$ MeV extracted from Ref. [8]. These data are in good agreement with our data and with the optical model calculation at forward angles.

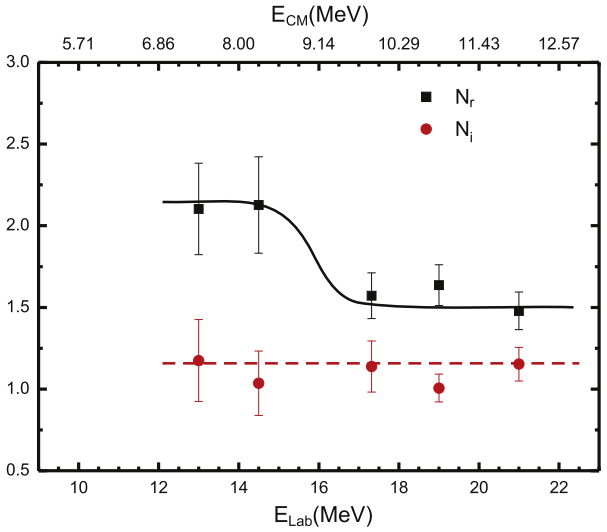

Fig. 3. (Color online.) Best values for N_r and N_i as a function of the bombarding energy obtained from fits using the São Paulo potential (Eq. (4)) for the $^{9}\mathrm{Be} + {}^{12}\mathrm{C}$ system. The lines are just to guide the eyes.

The N_r and N_i energy dependence is depicted in Fig. 3. The uncertainties are determined by a χ^2 analysis. One can notice that N_r increases in the vicinity of the Coulomb barrier energy ($E_{CM} \approx 9$ MeV [9,16]). The values of N_i are approximately constant for all energies, and they are in agreement with the results obtained in Ref. [17].

The increase of the N_r parameter near the Coulomb barrier suggests the presence of a threshold anomaly [18] However, no strong statement about this anomaly can be made due to the constant behavior of N_i.

The results from the first step of the analysis were used to perform the coupling of the inelastic and transfer channels presented in the next sections.

3.2. Inelastic channels

With the optical potentials previously obtained, we are able to take into account the effects of other channels. The second step of the analysis consisted in calculating the effects of inelastic channels in the theoretical elastic cross section, by considering $5/2^-$ and $7/2^-$ states of ^{9}Be and 2^+ of ^{12}C.

In our study the transitions to excited states of ^{9}Be and ^{12}C were calculated using the rotational model approach, where the coupling interaction $V_\lambda(\mathbf{r})$ of the multipole λ is

$$V_\lambda(\mathbf{r}) = -\delta_\lambda \frac{dV(\mathbf{r})}{dr}. \tag{5}$$

The Coulomb excitations are included by considering deformations on the charge distributions in the form

$$V_\lambda^C = M(\mathrm{E}\lambda)\frac{\sqrt{4\pi}e^2}{2\lambda+1}\begin{cases} r^\lambda/r_c^{2\lambda+1}, & r \leqslant r_c, \\ 1/r^\lambda, & r > r_c, \end{cases} \tag{6}$$

where

Table 1
Nuclear deformation parameters used in the inelastic calculations.

Nucleus	Transition	λ	$B(E\lambda)$	δ_λ
^{9}Be	$\frac{3}{2}^- \rightarrow \frac{5}{2}^-$	2	46.0 ± 0.5	2.4
^{9}Be	$\frac{3}{2}^- \rightarrow \frac{7}{2}^-$	2	33 ± 1	2.4
^{12}C	$0^+ \rightarrow 2^+$	2	42 ± 1	1.52

Table 2
Optical parameters for DWBA calculations and spectroscopic factor for a A = C + v system.

Systems	V_r (MeV)	r_r (fm)	a_r (fm)
^{9}Be + ^{9}Be[a]	189.3	1.0	0.63
^{3}He + ^{9}Be	55.8[b]	1.35	0.65
$A = C + v$	J^π	nlj	A
$^{12}C = {}^{9}Be \oplus {}^{3}He$	0^+	$2p_{3/2}$[c]	1.224[c]

[a] Refs. [20,21].
[b] Adjusted by FRESCO code to reproduce the cluster binding energy.
[c] Refs. [8,22].

$$M(E\lambda) = \sqrt{(2J_i + 1)B(E\lambda; J_i \rightarrow J_f)}. \tag{7}$$

Therefore, to take into account the effects of inelastic process in the theoretical elastic cross section, we take from the literature [8,9,19] the nuclear deformation parameters δ_λ and the reduced transition probabilities $B(E\lambda : J_i \rightarrow J_f)$, in order to calculate the deformations on the symmetrical central potential. The parameters for each channel included in the calculations and the reduced transition probabilities are presented in Table 1.

The results are shown as dashed lines in Fig. 2. In general, we observed that the inclusion of these channels decreases the theoretical cross section when compared to the results obtained only with the optical potential.

Comparing with the experimental data, we observed that the curves show a good description at forward angles. For intermediate and backward angles, the theoretical prediction underestimates the cross section. This demonstrates that the inclusion of these inelastic channels is not sufficient to explain the experimental results at intermediate and backward angles.

3.3. ^{3}He cluster transfer

In order to improve the description of experimental elastic distributions at intermediate and backward angular region, a coupling to the ^{3}He transfer was included in the third step of the analysis.

The calculations for ^{12}C(^{9}Be, ^{12}C)^{9}Be elastic transfer channel were done using the potential obtained in the optical model analysis. The ^{12}C was considered as a cluster structure, composed of a ^{9}Be core and a ^{3}He valence particle in a single-particle state. The bound state wave functions were generated using a binding potential with a Woods–Saxon shape, with geometric parameters shown in Table 2. The depth was adjusted to give the correct separation energy of the clusters.

In the calculation, ^{3}He is considered to be transferred from the $2p_{3/2}$ single particle state in $^{12}C(J^\pi = 0^+)$ to the same orbital on the $^{9}Be(J^\pi = 3/2^-)$ projectile. The spectroscopic factor for the $^{12}C_{g.s.} = {}^{9}Be_{g.s.} \oplus {}^{3}He$ cluster structure was taken from the literature and is listed in Table 2.

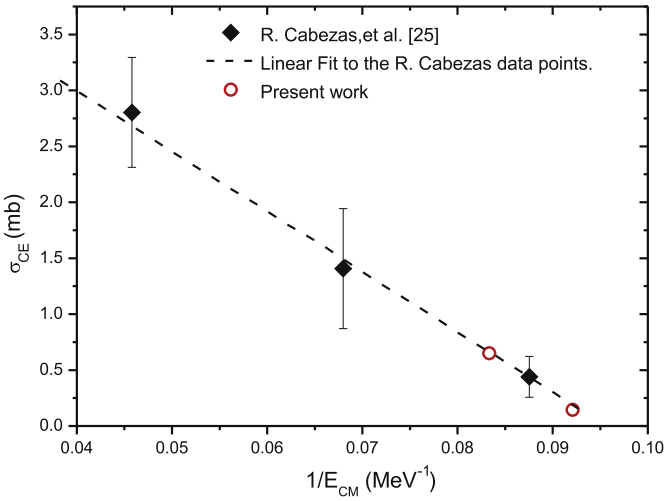

Fig. 4. (Color online.) Excitation function for compound nucleus formation. The open circle points are to $E_{Lab} = 19.0$ and 21.0 MeV. The calculated points, were normalized to agree with behavior of data from [23].

Table 3
Levels considered.

Residual nucleus	Level density parameter (MeV^{-1})[a]	Number of discrete levels
^{20}Ne	0.16	10
^{20}F	0.16	11
^{13}C	0.16	11
^{18}O	0.16	10
^{17}O	0.16	10
^{12}C	0.16	5

[a] Ref. [24].

The calculated angular distributions are shown in Fig. 2, as dash-dotted lines, and we can see the fair agreement with experimental data for 17.3, 19.0 and 21.0 MeV, showing the importance of the elastic transfer process at these energies. However, for 13.0 and 14.5 MeV, the importance of the inclusion of these channels is not clear. In the case of 19.0 MeV, one can notice that the theoretical prediction presents a good agreement when compared with the experimental data from Ref. [8].

3.4. Compound nucleus formation

The formation of compound nucleus is another mechanism that can also contribute to increase the cross sections at intermediate and forward angles [23,24]. Usually, in this process the nuclei fuse completely, forming an intermediate state ($^{9}Be + {}^{12}C \rightarrow {}^{21}Ne^{*}$), which after a characteristic time, decays populating other open channels, including the entrance channel. For the latter case we have the compound elastic (CE), which for $^{9}Be + {}^{12}C$ system is reflected in the process $^{9}Be + {}^{12}C \rightarrow {}^{21}Ne^{*} \rightarrow {}^{9}Be + {}^{12}C$.

The calculation was performed using the Hauser–Feshbach STATIS code [25]. The nuclear level density has been described by means of a level density expression given by Lang [26], and

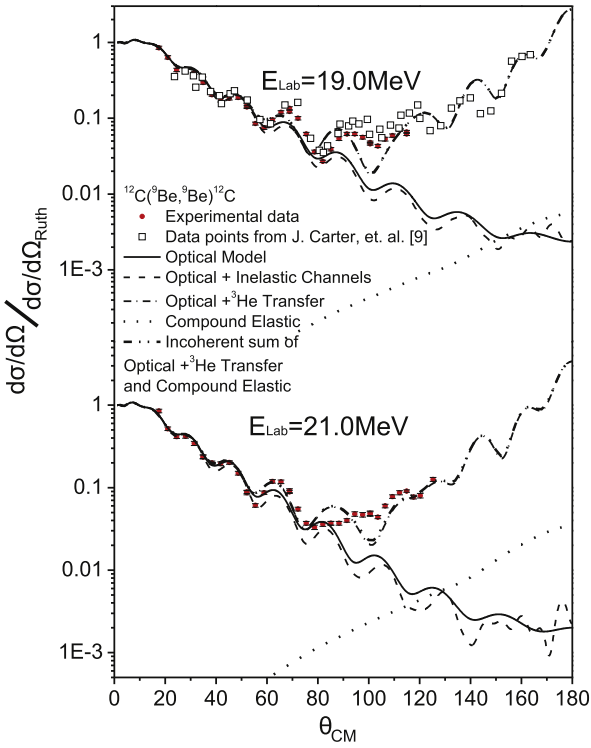

Fig. 5. (Color online.) Angular distributions for the $^{9}\mathrm{Be} + {}^{12}\mathrm{C}$ system at $E_{Lab} = 19.0$ and 21.0 MeV. The dot lines are the CE angular distributions from HF calculations. We can notice that the contribution of CE to differential cross section enhancement at backward angles is not significant.

the transmission coefficients were determined by an internal Fermi parametrization [25]. The levels considered in this calculations are listed on Table 3 and are quite similar to those used in Ref. [24].

Finally the angular distributions are normalized in such a way that the total cross section agree with the results presented in the excitation function from Ref. [23] (Fig. 4). When the obtained angular distributions are incoherently added to the ^{3}He transfer results, we can see that the contribution of this reaction mechanisms is not relevant, even for our highest energies, as shown in Fig. 5 for the two highest energies $E_{Lab} = 19.0$ and 21.0 MeV.

4. Conclusions

In this work we measured elastic scattering angular distributions for the $^{9}\mathrm{Be} + {}^{12}\mathrm{C}$ light system at bombarding energies ranging from 13.0 MeV to 21.0 MeV. The double folding São Paulo potential was used in the analysis that was performed in four steps.

In the first one we considered N_r and N_i as free parameters for the fits to the angular distributions at the forward angular region. The angular distributions calculated with the optical model have shown a good agreement with the 13.0 and 14.5 MeV experimental data. For 17.3, 19.0 and 21.0 MeV the agreement is reasonable at forward angles. However, the description at backward angles is not good, suggesting that the coupling to other mechanisms is important.

In the second step of the analysis, no evidence of the coupling to inelastic channels was observed. Using the spectroscopic factors extracted from the literature for $^{12}C = {}^{3}He \oplus {}^{9}Be$, in the third step we took into account the ^{3}He elastic transfer channel. For the ^{3}He transfer we see a pronounced improvement in the description of the data for 17.3, 19.0 and 21.0 MeV, which suggests that this process is important at intermediate and backward angles. Finally in the fourth step, corresponding to the compound elastic calculation, the results suggest that this mechanism is not an important process at the energies studied in this work.

The energy dependence of the N_r parameter suggest the presence of the threshold anomaly. However, no strong conclusions could be made due to the constant value of N_i.

Finally, to obtain information about the effects of the elastic transfer process and check the values of spectroscopic factors, it would be important to perform a more carefully analysis and measurements of the elastic scattering angular distributions at more backward angles.

References

[1] M. Dasgupta, D.J. Hinde, K. Hagino, Nucl. Phys. A 722 (2003) 196c.
[2] F.A. Souza, et al., Nucl. Phys. A 821 (2009) 36.
[3] L.F. Canto, P.R.S. Gomes, R. Donangelo, M.S. Hussein, Phys. Rep. 424 (2006) 1.
[4] C. Beck, N. Keeley, A. Diaz-Torres, Phys. Rev. C 75 (2007) 054605.
[5] A.M. Moro, F.M. Nunes, Nucl. Phys. A 767 (2006) 138.
[6] J.A. Tostevin, F.M. Nunes, I.J. Thompson, Phys. Rev. C 63 (2001) 024617.
[7] F.A. Souza, et al., Phys. Rev. C 75 (2007) 044601.
[8] J. Carter, et al., Nucl. Phys. A 591 (1995) 349.
[9] A.T. Rudchick, et al., Nucl. Phys. A 662 (2000) 44.
[10] W. von Oertzen, H.G. Bohlen, Phys. Rep. 19 (1975) 1.
[11] L.C. Chamon, et al., Phys. Rev. C 66 (2002) 014610.
[12] M.M. de Moura, et al., Nucl. Instrum. Methods A 471 (2001) 368.
[13] I.J. Thompson, Comp. Phys. Rep. 7 (1988) 167.
[14] D. Pereira, et al., Phys. Lett. B 670 (2009) 330.
[15] D.P. Souza, et al., Nucl. Phys. A 836 (2010) 1.
[16] A.T. Rudchik, et al., Nucl. Phys. A 660 (1999) 267.
[17] A. Barioni, et al., Phys. Rev. C 80 (2009) 034617.
[18] M.S. Hussein, P.R.S. Gomes, J. Lubian, L.C. Chamon, Phys. Rev. C 73 (2006) 044610.
[19] D.R. Tilley, et al., Nucl. Phys. A 745 (2004) 155.
[20] R.C. York, R.T. Carpenter, Nucl. Phys. A 282 (1977) 351.
[21] E. Ungricht, et al., Nucl. Phys. A 313 (1979) 376.
[22] A.T. Rudchik, et al., Nucl. Phys. A 667 (2000) 61.
[23] R. Cabezas, et al., Phys. Rev. C 60 (1999) 067602.
[24] J.F. Mateja, et al., Phys Rev. C 20 (1979) 176.
[25] R.G. Stokstad, Internal report 52, STATIS Program, Wright Nuclear Structure Laboratory, Yale University, 1972.
[26] D.W. Lang, Nucl. Phys. 42 (1963) 353.